ELECTROMAGNETIC MODELING OF BEAM POSITION AND PHASE MONITORS FOR THE LANSCE LINAC*

Sergey S. Kurennoy#, LANL, Los Alamos, NM 87545, U.S.A.

Abstract

Electromagnetic modeling has been used to compare designs of pickups for the beam position and phase monitors (BPPM) for the Los Alamos Neutron Science Center (LANSCE) linac. This study is a part of the efforts to upgrade LANSCE beam diagnostics [1]. MAFIA 3-D time-domain simulations with an ultra-relativistic beam allow computing the signal amplitudes and phases on the BPPM electrodes for the given processing frequency, 201.25 MHz, as functions of the beam transverse position. An analytical model can be applied to extrapolate the simulation results to lower beam velocities. Based on modeling results, a BPPM design with 4 one-end-shorted electrodes each covering 60-degree subtended angle, similar to the SNS linac BPPM [2], appears to provide the best combination of mechanical and diagnostics properties for the LANSCE side-coupled linac.

INTRODUCTION

The paper studies physical aspects of the pickup design for 4-electrode beam position and phase monitors (BPPM) in the LANSCE proton linac. The BPPMs are planned to be installed in the 805-MHz coupled-cavity part of the linac that starts at the beam energy 100 MeV. Within usual geometrical limitations – the available longitudinal space for the BPPM is limited to 2-3″ – we compare two main design options. The first one is a recessed stripline design with two 50-Ω coaxial connectors at both ends, similar to the LANSCE IPF BPM, e.g., see [3]. The other design employs one-end-shorted striplines having one 50-Ω connector at the other end, like in the SNS linac BPM [2]. The BPPM transverse cross sections (one-quarter) are shown in Fig. 1, 3D views in Fig. 2. For comparison we assume the same electrode length (L = 40 mm) and subtended angle ($\varphi = 60°$) in both designs, and choose the same beam pipe inner radius b = 19 mm (diameter ≈1.5″).

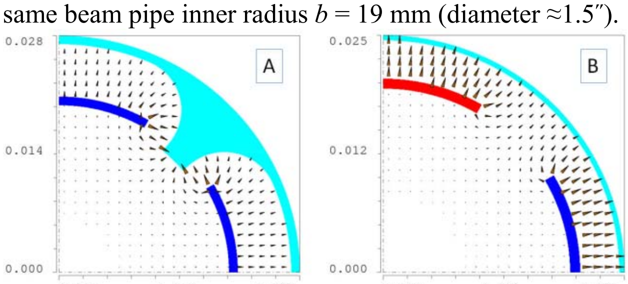

Figure 1: Cross sections (1/4) of the recessed stripline (A) and simple stripline (B) BPPM. Dimensions are in m. The BPPM box is in light-blue. Arrows show electrostatic fields for equal voltages on the electrodes.

The electrode thickness is 1 mm in both cases, and the recess depth (design A) is 1 mm radially. We will also consider a trade-off design C that has recessed electrodes as in A but shorted at one end, as in B, where the lobes are flush with the beam pipe. Engineering considerations somewhat favor design B (or C) as a simpler and more robust one [4]; it is also cheaper due to a smaller number of connectors. For the same reason, such BPMs are easier to install in tight spots. One the other hand, in design A the lobe-to-lobe coupling is smaller, and there has been plenty of good experience in using them at LANL.

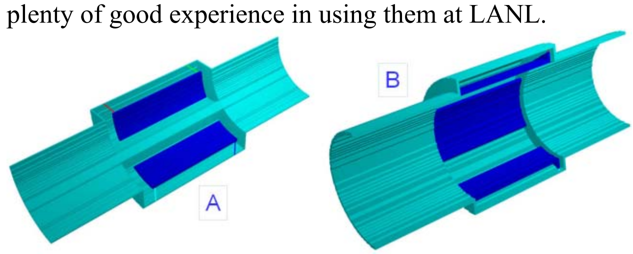

Figure 2: 3D views of BPPM design A (1/4 is shown) and B (1/2 cut). Connectors are shown by thin colored lines.

MAFIA MODELING OF BPPM

The characteristic impedances Z_c of transmission lines formed by the lobes are computed in the static limit in 2D with the MAFIA code, and the cross-section geometry is adjusted to provide Z_c = 50 Ω. This corresponds to the BPM matching to the sum mode, which is sufficient for the proposed narrow-band signal processing at the linac bunch repetition frequency f_b = 201.25 MHz. For the broad-band signal processing including higher harmonics, matching to the dipole mode would be advantageous [5].

We use 3-D simulations with the MAFIA time-domain module T3 to compute voltages induced on the BPPM electrodes by an ultra-relativistic linac bunch. The bunch is simulated in T3 by a line charge Q = 65 pC having a Gaussian longitudinal distribution with rms length σ_z = 5 mm traveling parallel to the BPM axis ($x = 0$, $y = 0$) with velocity $v = c$ ($\beta = 1$). This bunch charge corresponds to the average macropulse current of 13 mA. The voltages are recorded during the bunch repetition period $T = 1/f_b$ = 4.969 ns, or for cT = 1.49 m. The β-correction (see references in [2]) to the signal voltages can be neglected here: the correction factor is 0.99 even at the lowest beam energy in the LANSCE side-coupled linac, about 100 MeV (β = 0.43). From the voltage signals computed in time domain we find the amplitudes and phases of the signal harmonics at multiples of f_b as functions of the beam transverse position. The signal amplitudes and phases on individual electrodes for the given processing frequency depend on the beam transverse position, while the amplitude and phase of the summed signal is practically independent of it, see in [2, 6].

* This work was supported by the US Department of Energy under Contract Number DE-AC52-06NA25396
#kurennoy@lanl.gov

Beam Position Performance

Figure 3 shows the Fourier-transform amplitudes of the voltage signals induced on different electrodes – marked R, T, L, B for right, top, left, bottom – versus frequency in the case of the beam transverse displacement x/b = 0.25, y/b = 0.125 compared to those for an on-axis beam (‘*cb*’). These plots help compare the high-frequency behavior: obviously, the resonances start at the lower frequencies in the design A. For the position and phase processing in the LANSCE linac, we are only interested in the fundamental (n = 1) harmonic at the signal processing frequency $f = f_b$ = 201.25 MHz – the left-most group of data points.

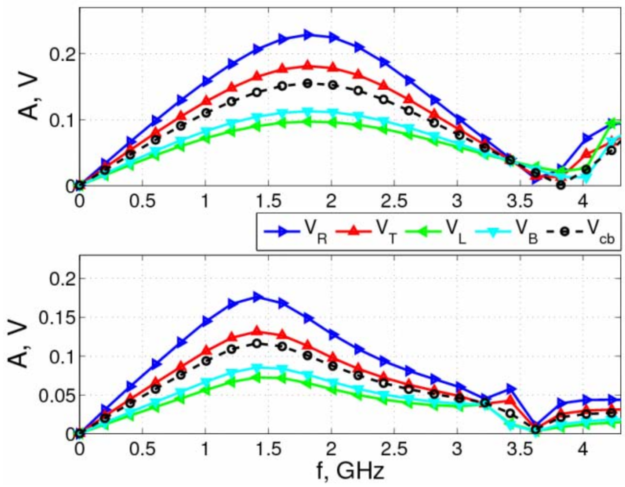

Figure 3: Harmonics of electrode signals in BPPM design B (top) and A (bottom) – see explanations in the text.

The amplitudes A and power P of the fundamental harmonic of the signal voltage Fourier-transform from an on-axis beam in the three BPPM designs are listed in Tab. 1. It also gives the minimal power P_{min} and the signal power range ΔP for the beam transverse deflection from the axis within the square aperture of $-b/2 < x,y < b/2$, as well as the average BPM sensitivity S. One should remind that the power values P and P_{min} in Tab. 1 are computed at 13 mA. The LANSCE average macropulse current ranges from 1 to 20 mA, and for the low current in the linac, 1 mA, these values are further reduced by 22.3 dB.

Table 1: Signal parameters in BPPM pickups at $f = f_b$

Design type	A, mV	P, dBm	P_{min}, dBm	ΔP, dB	S, dB/mm
A	20.0	-24.0	-36.3	20.3	1.70
B	23.7	-22.5	-32.3	16.4	1.39
C	19.0	-24.4	-34.9	17.5	1.51

While the signal amplitudes on electrodes change significantly depending on the beam transverse position, the amplitude of their sum signal A_Σ remains quite stable. Therefore, the sum signal can be used to reliably measure the beam current. The A_Σ variations are smaller in the design B: its deviation from the average is less than 3% of the average, while it is about 7% for the cases A and C.

Electrode Coupling and Cross-Plane Correlation in Beam Position Measurements

To find the coupling between BPPM electrodes, we excite the BPM structure by feeding one electrode with a signal at 201.25 MHz with its voltage amplitude increasing to some final value V_1, and find – using 3D MAFIA time-domain simulations – the voltages induced on other electrodes. The dynamic coupling coefficients are defined as ratios of these amplitudes to that of the exciting signal: $k_{12}=V_2/V_1$ for the adjacent electrode, and $k_{13}=V_3/V_1$ for the opposite electrode. The results are presented in Tab. 2. As a cross-check, we performed MAFIA simulations with broadband pulses centered at 201.25 MHz, and also using MicroWave Studio for the design B; the results were very close to those in Tab. 2.

Table 2: Electrode dynamic coupling coefficients

BPPM Design	A	B	C
Coupling k_{12}	$4.30\cdot10^{-3}$	$4.35\cdot10^{-2}$	$1.35\cdot10^{-2}$
Coupling k_{13}	$1.54\cdot10^{-3}$	$1.38\cdot10^{-2}$	$4.79\cdot10^{-3}$

As expected, the design A with 2-connector recessed electrodes that are separated by the grounded insertions of the BPM-box wall, see Fig. 1, has the lowest coupling between electrodes. In the design C, shorting one end of the recessed electrodes increases the coupling about 3 times compared to A. The design B has the highest electrode-to-electrode coupling, an order of magnitude higher than A.

However, a large electrode-to-electrode coupling does not necessarily mean that the results of beam position measurements in one plane will be strongly influenced by the beam position in the orthogonal plane. To compare such cross-plane correlations for the three BPM designs, Tab. 3 lists P_R-P_L = 20 $\log_{10}(A_R/A_L)$ – the difference of the signal power from the right and left electrodes – with two beam horizontal deflections, $x = b/4$ and $x = b/2$, for different vertical deflections y. Ideally, if there were no cross-plane correlation, the difference P_R-P_L would depend only on x, not on y.

Table 3: P_R-P_L (dB) versus beam position at $f = f_b$

x/b	y/b	A	B	C
0	0	0	0	0
0.25	0	8.27	6.45	7.65
0.25	0.125	8.25	6.44	7.59
0.25	0.25	8.19	6.39	7.38
0.5	0	16.10	14.04	15.17
0.5	0.25	16.17	14.05	14.89
0.5	0.5	15.76	13.49	13.28

As one can see, the y-dependence is the strongest for the design C, while it is much weaker in the design B. Design B turns out to be as good as A, or even slightly better, in that respect, for small beam displacements from the axis. This is an important point, worth to be emphasized again: *the electrode-to-electrode coupling in BPPMs is not directly related to the cross-plane correlations in beam position measurements*, as can be proved by comparison of Tab. 2 and 3.

One the other hand, the BPM linearity is smaller in the design A than in B. In fact, the design C gives the most linear reading in the horizontal plane, but its cross-plane dependence is too strong. Both non-linearities and cross-plane correlations can be addressing with a proper 2D BPM mapping. However, minimizing cross-correlations is more important because it also reduces the effects of the beam transverse charge distribution on the beam position measurements. This is due to the fact that the beam-size effects in the lowest order enter only via the combination y^2-M_2, where M_2 is the second moment of the beam-charge transverse distribution, cf. [7].

Beam Phase Performance

The phases of the fundamental harmonic of the voltages induced on the individual electrodes of the BPPM design B (with respect to the phase of the sum signal from all electrodes, φ_Σ) are summarized in Tab. 4. Table 4 also gives the phase difference $\Delta\varphi = \varphi_\Sigma - \varphi_{cb}$ between the sum-signal phase and the phase of the same beam traveling on axis, the centered beam.

Table 4: Phases of the signal fundamental harmonic for the BPPM design B versus beam transverse position

x/b	y/b	φ_R φ_L φ_T φ_B,°	φ_Σ,°	$\Delta\varphi$,°
0	0	0	-109.18	0
0.25	0	0.86 -0.18 -1.31 -0.18	-109.19	0.00
0.25	0.125	0.83 0.38 -1.38 -0.89	-109.18	0.00
0.25	0.25	0.76 0.76 -1.58 -1.58	-109.17	0.01
0.5	0	1.49 -1.04 -3.82 -1.04	-109.22	-0.04
0.5	0.25	1.41 0.26 -4.09 -2.82	-109.17	0.01
0.5	0.5	1.18 1.18 -5.59 -5.59	-108.99	0.19

The 3D MAFIA time-domain runs were performed with a relatively crude cubic mesh having steps $d = 0.5$ mm in all three dimensions, so they cannot resolve time differences shorter than $\Delta t \approx d/c = 1.7$ ps. This time uncertainty corresponds to 0.12° of the RF phase at 201.25 MHz, which gives an estimated accuracy of our simulations. For large beam deflections the signal phases from different electrodes can differ by about 7° in Tab. 4, much larger than the estimated accuracy. The difference is even larger in design A, 11°, and reaches 16° in C. However, the sum-signal phase remains independent of the beam position and equal to the centered-beam phase within the estimated accuracy. One possible exception is for rather extreme beam deflection, half-aperture in both planes; it is highlighted in the last row. This independence on the beam position [6] provides a base for reliable phase measurements with BPPMs using the sum signal.

CONCLUSION

Three designs for the beam position and phase monitors (BPPM) in the LANSCE linac were compared using 3D MAFIA electromagnetic simulations. We conclude that two designs, A with recessed 2-connector electrodes, and B with flush one-end-shorted electrodes, can successfully satisfy the beam diagnostics requirements [1] for the LANSCE linac. In fact, even the trade-off design C is acceptable; it just has larger cross-plane correlations.

Both designs, A and B, have their advantages and disadvantages. Design A has smaller non-linearities and higher position sensitivity. Design B provides more signal power, has low cross-plain correlations and better high-frequency characteristics. The choice should be made based on engineering and cost considerations. Due to the smaller number of the RF connectors, 4 versus 8, the BPPM type B is cheaper than A. Its mechanical design is simple and more robust, see [4]. For the same electrode length, the pickup B is shorter by 2-3 mm (one gap instead of two in A). The pickup box radius is smaller for the BPPM type B, and generally, this pickup is easier to install into tight spots. Due to these reasons, the BPPM design B was chosen for the LANSCE linac.

The LANSCE linac BPPMs will be installed between the tanks of the side-coupled linac where the beam pipe has inner diameter of 1.745″. MAFIA modeling of the BPPM type B with this larger bore (b = 22.16 mm) has been performed. The pickup physical characteristics are very similar to those for the type B above. One change – the lower sensitivity in the position measurements, 1.26 dB/mm instead of 1.39, cf. Tab. 1 – was expected since the sensitivity scales approximately as $1/b$.

The author would like to acknowledge useful discussions with and advice from J.D. Gilpatrick, J.F. O'Hara, and J.F. Power of LANL.

REFERENCES

[1] J.D. Gilpatrick, et al., "Proposed Beam Diagnostics Instrumentation for the LANSCE Refurbishment Project," these proceedings.

[2] S.S. Kurennoy and R.E. Shafer, "Electromagnetic Modeling of Beam Position Monitors for SNS Linac," EPAC 2000, Vienna, Austria, p. 1768.

[3] S.S. Kurennoy, "EM analysis of wide-lobe BPMs for the IPF," tech note LANSCE-1: 99-150, Los Alamos, 1999.

[4] J.F. O'Hara, et al., "LANSCE Prototype Beam Position and Phase Monitor (BPPM) Mechanical Design," these proceedings.

[5] C. Deibele and S. Kurennoy, "Matching BPM Stripline Electrodes to Cables and Electronics" PAC 2005, Knoxville, TN, p. 2607.

[6] S.S. Kurennoy, "Beam Phase Detectors for Spallation Neutron Source Linac," EPAC 2000, Vienna, Austria, p. 1765.

[7] S.S. Kurennoy, *Physical Review ST Accel. Beams*, 4, 092801 (2001); 6, 039902 (2003).